Acta Crystallographica Section B
Structural Science
ISSN 0108-7681

Crystallographic and molecular mechanics investigation of an order–disorder transition and dimorphism in 5*H*,10*H*-dithiolo[2,3-*b*]-2,5-benzodithiocine-2-thione

Zahid H. Chohan, William T. A. Harrison, R. Alan Howie, Bruce F. Milne and James L. Wardell*

Department of Chemistry, University of Aberdeen, Old Aberdeen AB24 3UE, Scotland

Correspondence e-mail: j.wardell@abdn.ac.uk

Received 24 February 2000
Accepted 28 July 2000

Single-crystal X-ray structures are presented for three forms of 5*H*,10*H*-dithiolo[2,3-*b*]-2,5-benzodithiocine-2-thione. The α (at 150 K) and α' (at ambient) forms are very similar and differ only in the presence of crystallographic *m* symmetry in the molecules of α', which is absent in the case of α. This pair is related by an order–disorder transition. The β phase (also determined at 150 K) has a different structure in terms of the molecular packing from either of the other two and therefore constitutes a true polymorph. Molecular mechanics calculations indicated that the most stable $CHCl_3$-solvated conformations for the title compound were a pair of twisted *U*-shaped enantiomers, U_R and U_L, *i.e.* similar to the arrangements found in the α and β phases, with the low-lying saddle point between them corresponding to the situation in the α' phase. These calculations also indicated that the most stable $CHCl_3$-solvated conformation for the related dibromo-5*H*,10*H*-dithiolo[2,3-*b*]-2,5-benzodithiocine-2-thione was *Z*-shaped, in agreement with the crystal structure determined earlier for its DMSO solvate [Wang *et al.* (1998). *Synthesis*, pp. 1615–1618].

1. Introduction

The packing of molecules in the crystalline state has a crucial bearing on their material properties. Various types of intermolecular and interion interactions can help fashion the solid-state assembly (Desiraju, 1995). In aromatic and other π-delocalized systems, π–π interactions are particularly important intermolecular forces (Hunter, 1994). For derivatives of 4,5-dimercapto-1,3-dithiole-2-thione [H_2-dmit: (1)], the frequently reported non-covalent intermolecular and interionic interactions are S···S contacts, as illustrated by the dmit compounds listed in the Cambridge Structural Database (Allen & Kennard, 1993; Fletcher *et al.*, 1995). As part of an ongoing study on dmit compounds, the structure of 5*H*,10*H*-dithiole[2,3-*b*]-2,5-benzodithiocine-2-thione (2) was determined at ambient temperature; surprisingly, this was found to have a *U*-shaped molecular structure in contrast to the *Z*-shaped structures established for the solvates of related compounds (3) [(3):DMSO] and (4) [(4):DMF] (Wang *et al.*, 1998). This finding led us onto a molecular mechanics study of (2) and (3), and the determination of structures at 150 K of (2)

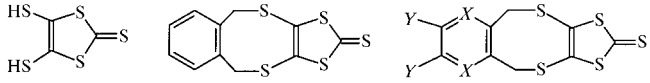

(1) (2) (3): X = CH; Y = Br (4): X = N; Y = CN

recrystallized from different media. As we now report, the study revealed an order–disorder relationship and dimorphism in (2).

Table 1
Experimental details.

	α-(2)	α'-(2)	β-(2)
Crystal data			
Chemical formula	$C_{11}H_8S_5$	$C_{11}H_8S_5$	$C_{11}H_8S_5$
Chemical formula weight	300.47	300.47	300.47
Cell setting	Monoclinic	Monoclinic	Monoclinic
Space group	$P2_1/a$	$C2/m$	$P2_1/n$
a (Å)	11.9290 (2)	12.075 (8)	8.5683 (2)
b (Å)	11.7639 (2)	11.825 (8)	16.2080 (4)
c (Å)	9.0612 (2)	9.063 (6)	17.8980 (4)
β (°)	103.9498 (10)	102.80 (5)	97.1103 (14)
V (Å^3)	1234.07 (4)	1261.9 (15)	2466.47 (10)
Z	4	4	8
D_x (Mg m^{-3})	1.617	1.582	1.618
Radiation type	Mo $K\alpha$	Mo $K\alpha$	Mo $K\alpha$
Wavelength (Å)	0.71073	0.71073	0.71073
No. of reflections for cell parameters	21 934	14	31 494
θ range (°)	2.32–27.46	10.8–12.9	1.70–26.43
μ (mm^{-1})	0.905	0.885	0.905
Temperature (K)	150 (2)	298 (2)	150 (2)
Crystal form	Block	Block	Block
Crystal size (mm)	0.30 × 0.20 × 0.20	0.60 × 0.46 × 0.40	0.20 × 0.10 × 0.10
Crystal colour	Red	Pale brown	Orange
Data collection			
Diffractometer	Enraf–Nonius KappaCCD area detector	Nicolet P3	Enraf–Nonius KappaCCD area detector
Data collection method	ω scans	θ–2θ scans	ω scans
Absorption correction	Multi-scan	ψ	Multi-scan
T_{min}	0.728	0.619	0.809
T_{max}	0.835	0.719	0.914
No. of measured reflections	21 934	2034	31 494
No. of independent reflections	2825	1932	5044
No. of observed reflections	2500	1166	3825
Criterion for observed reflections	$I > 2\sigma(I)$	$I > 2\sigma(I)$	$I > 2\sigma(I)$
R_{int}	0.0472	0.0238	0.0734
θ_{max} (°)	27.46	30.09	26.43
Range of h, k, l	$-15 \rightarrow h \rightarrow 15$ $-15 \rightarrow k \rightarrow 15$ $-11 \rightarrow l \rightarrow 11$	$-16 \rightarrow h \rightarrow 16$ $-16 \rightarrow k \rightarrow 0$ $0 \rightarrow l \rightarrow 12$	$-10 \rightarrow h \rightarrow 10$ $-20 \rightarrow k \rightarrow 20$ $-22 \rightarrow l \rightarrow 22$
No. of standard reflections	–	2	–
Frequency of standard reflections	–	Every 50 reflections	–
Refinement			
Refinement on	F^2	F^2	F^2
$R[F^2>2\sigma(F^2)]$	0.0278	0.0862	0.0363
$wR(F^2)$	0.0712	0.2153	0.0918
S	1.051	1.053	1.032
No. of reflections used in refinement	2825	1932	5044
No. of parameters used	145	78	289
H-atom treatment	H-atom parameters constrained	Only H-atom U's refined	H-atom parameters constrained
Weighting scheme	$w = 1/[\sigma^2(F_o^2) + (0.0370P)^2 + 0.4749P]$, where $P = (F_o^2 + 2F_c^2)/3$	$w = 1/[\sigma^2(F_o^2) + (0.0535P)^2 + 8.1837P]$, where $P = (F_o^2 + 2F_c^2)/3$	$w = 1/[\sigma^2(F_o^2) + (0.0422P)^2 + 0.3638P]$, where $P = (F_o^2 + 2F_c^2)/3$
$(\Delta/\sigma)_{max}$	0.001	0.000	0.001
$\Delta\rho_{max}$ (e Å^{-3})	0.38	0.92	0.45
$\Delta\rho_{min}$ (e Å^{-3})	−0.38	−0.95	−0.29
Extinction method	None	None	None
Source of atomic scattering factors	*International Tables for Crystallography* (1992, Vol. C, Tables 4.2.6.8 and 6.1.1.4)	*International Tables for Crystallography* (1992, Vol. C, Tables 4.2.6.8 and 6.1.1.4)	*International Tables for Crystallography* (1992, Vol. C, Tables 4.2.6.8 and 6.1.1.4)
Computer programs			
Data collection	*DENZO* (Otwinowski & Minor, 1997), *COLLECT* (Hooft, 1998)	*P*3 software (Nicolet, 1980)	*DENZO* (Otwinowski & Minor, 1997), *COLLECT* (Hooft, 1998)
Cell refinement	*DENZO* (Otwinowski & Minor, 1997), *COLLECT* (Hooft, 1998)	*P*3 software (Nicolet, 1980)	*DENZO* (Otwinowski & Minor, 1997), *COLLECT* (Hooft, 1998)

Table 1 (continued)

	α-(2)	α'-(2)	β-(2)
Data reduction	*DENZO* (Otwinowski & Minor, 1997), *COLLECT* (Hooft, 1998)	*RDNIC* (Howie, 1980)	*DENZO* (Otwinowski & Minor, 1997), *COLLECT* (Hooft, 1998)
Structure solution	*SHELXS*97 (Sheldrick, 1990)	*SHELXS*97 (Sheldrick, 1990)	*SHELXS*97 (Sheldrick, 1990)
Structure refinement	*SHELXL*97 (Sheldrick, 1997)	*SHELXS*97 (Sheldrick, 1990)	*SHELXS*97 (Sheldrick, 1990)
Preparation of material for publication	*SHELXS*97 (Sheldrick, 1990)	*SHELXS*97 (Sheldrick, 1990)	*SHELXS*97 (Sheldrick, 1990)

2. Experimental

2.1. General techniques

Melting points were measured on a Kofler hot-stage microscope and are uncorrected. NMR spectra were recorded on Bruker 250 MHz and 400 MHz instruments, UV–vis spectra on a Perkin Elmer Lambda 15 instrument and IR spectra on a Philips Analytical PU9800 FTIR instrument. Differential scanning calorimetry was carried out on a DSC Metler Toledo 820 instrument. The compound $[NEt_4]_2[Zn(dmit)_2]$ was obtained by a published procedure (Wang *et al.*, 1998).

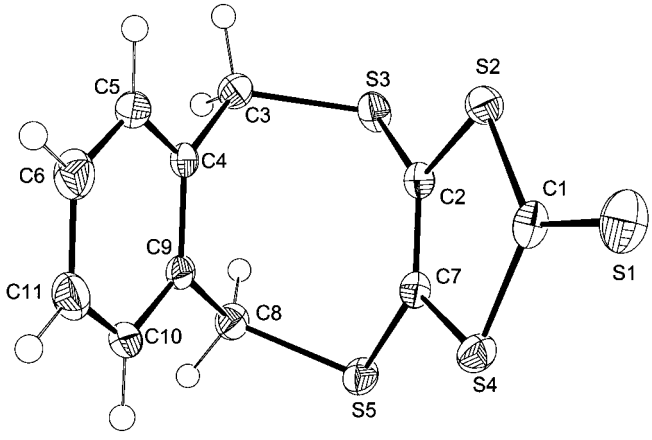

Figure 1
Atom-labelling scheme for α-(2) (50% probability displacement ellipsoids). H atoms represented by plain spheres of arbitrary radius.

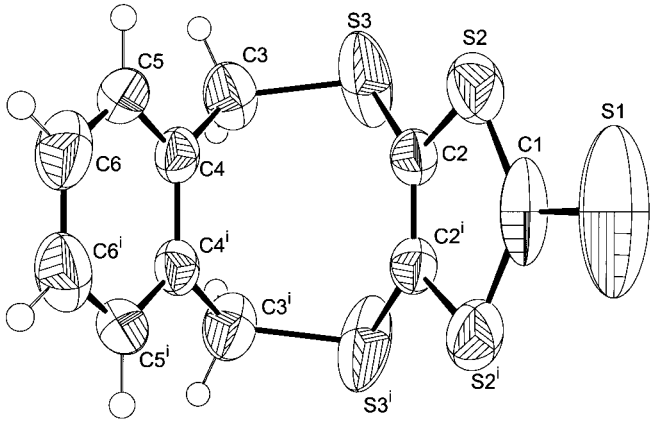

Figure 2
Atom-labelling scheme for α'-(2) (50% probability displacement ellipsoids). H atoms represented by plain spheres of arbitrary radius. Symmetry code: (i) $x, -y, z$.

2.2. Synthesis

Solutions of 1,2-bis(chloromethyl)benzene (0.88 g, 5.0 mmol) in CH_2Cl_2 (20 ml) and $[NEt_4]_2[Zn(dmit)_2]$ (1.80 g, 2.50 mmol) in CH_2Cl_2 (30 ml) were mixed and refluxed overnight. The solvent was removed to leave an oil, which was chromatographed on silica using CH_2Cl_2 as an eluent. The title compound was recrystallized from CH_2Cl_2/hexane as a red crystalline solid (polymorph α), m.p. 479 K [literature values 478 K (Kumar *et al.*, 1991), 480 K (Goldenberg & Lyubovskaya, 1986)]; yield 0.78 g, 52%. Recrystallization from DMF and $CHCl_3$ also gave polymorph α. Analysis: found: C 43.1, H 2.5%; calculated for $C_{11}H_8S_5$: C 43.2, H 2.7%. IR (KBr): ν(C═S) 1066 cm^{-1}. UV–vis (CH_2Cl_2): 374, 520 nm. ^{13}C NMR ($CDCl_3$, 63 MHz): δ 38.6 [CH_2], 129.0 [C4], 130.7 [C3], 134.0 [C1], 139.3 [C═C], 211.8 [C═S].

Crystallization of the residue of a reaction mixture also containing $Cr(CO)_6$ from ethanol gave the orange β phase, m.p. 479–480 K, whose solution NMR and solid-state IR spectral data were identical with those of the α' phase.

2.3. Molecular mechanics calculations

The calculation of the minimum energy solution ($CHCl_3$) conformations of (2) and (3) was carried out using Macromodel v6.5 (Mohamadi *et al.*, 1990) on a Silicon Graphics O2 workstation. Monte Carlo searching of the conformational spaces accessible to the two molecules was performed with subsequent Polak–Ribere conjugate gradient energy minimization of the generated structures. The MM2* force-field was employed for all energy calculations along with the GB/SA solvent model (Still *et al.*, 1990) using non-bonded cutoffs of 12 Å for electrostatic interactions and 7 Å for van der Waals' interactions.

2.4. Crystallography

Intensity data for α-(2) and β-(2) were collected at 150 K on an Enraf–Nonius KappaCCD area detector diffractometer, as outlined in Table 1.[1] Room-temperature data for α'-(2) were collected on a Nicolet P3 diffractometer (Table 1). For α-(2) and β-(2), absorption corrections were made on the basis of multiply measured and symmetry-equivalent reflections using *SORTAV* (Blessing, 1997), while ψ scans were applied to the data for α'-(2).

[1] Supplementary data for this paper are available from the IUCr electronic archives (Reference: BM0027). Services for accessing these data are described at the back of the journal.

Each structure was solved by direct methods with *SHELXS*86 (Sheldrick, 1990) and optimized by full-matrix least-squares refinement against F^2 by using *SHELXL*97 (Sheldrick, 1997). H-atom locations were calculated geometrically and thereafter allowed to ride on their respective C atoms. For the α and β phases, U_{iso} for each H was set to 1.2 × U_{eq} of its attached C. For the α' phase, separate common group U_{iso} values were refined for methylene and aryl H.

3. Results and discussion

3.1. General

Compound (2) was obtained from the reaction between $[NEt_4]_2[Zn(dmit)_2]$ and 1,2-$(ClCH_2)_2C_6H_4$ in CH_2Cl_2 solution. Recrystallization from CH_2Cl_2, DMF or CH_2Cl_2/EtOH gave the same product, designated the α' phase, from structure determinations at 298 (2) K, and the α phase, from structure determinations at 150 (2) K. In contrast to (3), (2) did not form a DMF solvate on recrystallization from DMF solution. DSC experiments with the α/α' material indicated a very weak (0.42 kJ mol^{-1}), but reproducible endothermic event at 249 K either on cooling from 330 K or heating from 170 K. This thermal behaviour is consistent with a subtle molecular rearrangement on going from the α to the α' form of (2) (see below). The β phase, determined at 150 K, was obtained from a reaction mixture of (2) and $Cr(CO)_6$. The role of the chromium hexacarbonyl is unknown at this stage.

The atom-labelling schemes of α-(2) and α'-(2) are shown in Figs. 1 and 2. The atom-labelling scheme of α-(2) is also used for β-(2) with the additional use of suffixes *a* and *b* to identify the two independent molecules (Figs. 3 and 4). Selected bond distances and angles are listed in Table 2. These molecules have '*U*'-shaped structures, with the benzene ring and the dmit moiety as the legs of the '*U*' and the methylene C atoms and the attached S atoms as its base. The *U*-shaped structures are significantly different from the *Z*-shaped structures of the compounds (3):DMSO and (4):DMF (Wang *et al.*, 1998).

3.2. Molecular mechanics results

These calculations indicated five minima, as listed in Table 3. These minima corresponded to two enantiomeric and, therefore, equal-energied, twisted *U*-shaped conformations, U_L and U_R, a *Z*-shaped conformation and an enantiomeric pair of irregular conformations, T_L and T_R. The most stable $CHCl_3$-solvated conformation calculated for (3) is the *Z*-form, *i.e.* the conformation determined for the solid DMSO-solvate of (3). For molecule (2), the lowest energy conformations are, however, calculated to be the pair of enantiomers U_L and U_R, *i.e.* similar to the arrangements found in α-(2) and β-(2), with the low-lying saddle point between them corresponding to the situation in α'-(2), see below. The highest energy conformations, T_L and T_R, are twist forms in which the 'hinge' exocyclic S atoms lie one above and one below the phenyl ring: the angle between the planes of the phenyl ring and dmit ring is 61.6°.

The potential energy surface was investigated for the presence of saddle points lying between the minima using the *Macromodel* explicit saddle point search method (Culot *et al.*, 1990). Three saddle points (Table 4) were found to lie between true minima on the surface: (i) between U_L and U_R (a regular *U* shape) and (ii) two equal energy sites between U_L and T_L, and between U_R and T_R. Another saddle point was found to be

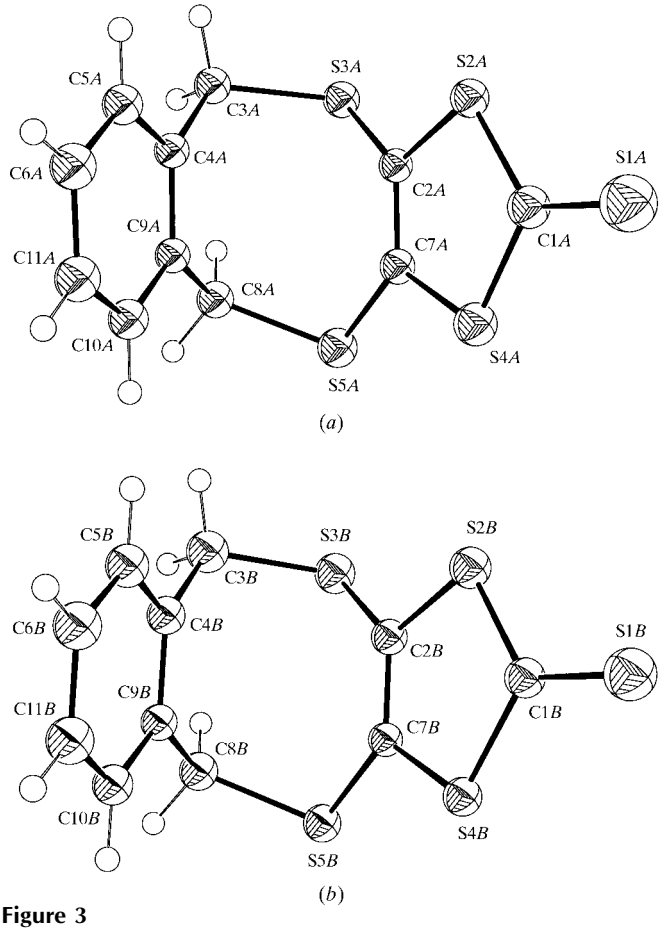

Figure 3
Atom-labelling scheme for (*a*) molecule *A* of β-(2) and (*b*) molecule *B* of β-(2) (50% probability displacement ellipsoids in each case). H atoms represented by plain spheres of arbitrary radius.

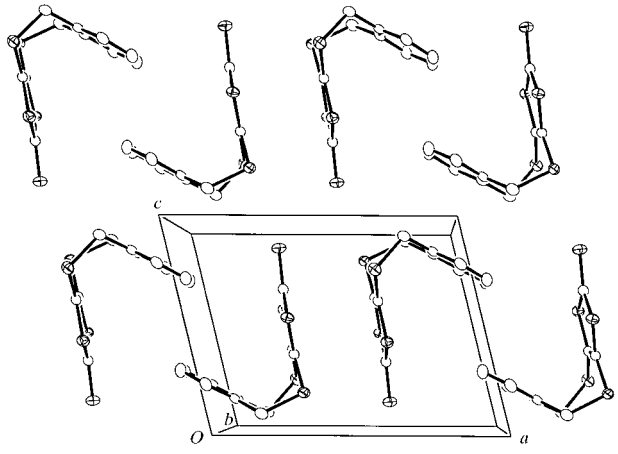

Figure 4
Packing-diagram for α-(2)

Table 2
Selected geometric parameters (Å, °).

α-2			
S1—C1	1.6400 (15)	C2—C7	1.354 (2)
S2—C1	1.7324 (16)	C3—C4	1.502 (2)
S2—C2	1.7449 (15)	C4—C5	1.393 (2)
S3—C2	1.7436 (14)	C4—C9	1.403 (2)
S3—C3	1.8477 (16)	C5—C6	1.383 (2)
S4—C1	1.7416 (17)	C6—C11	1.391 (3)
S4—C7	1.7442 (15)	C8—C9	1.498 (2)
S5—C7	1.7466 (15)	C9—C10	1.391 (2)
S5—C8	1.8468 (16)	C10—C11	1.383 (2)
C1—S2—C2	98.01 (7)	C9—C4—C3	122.86 (13)
C2—S3—C3	102.93 (7)	C6—C5—C4	121.47 (15)
C1—S4—C7	98.17 (7)	C5—C6—C11	119.57 (15)
C7—S5—C8	102.55 (7)	C2—C7—S4	115.53 (11)
S1—C1—S2	125.54 (10)	C2—C7—S5	128.61 (12)
S1—C1—S4	122.65 (10)	S4—C7—S5	115.85 (9)
S2—C1—S4	111.81 (8)	C9—C8—S5	111.76 (10)
C7—C2—S3	124.76 (12)	C10—C9—C4	119.20 (13)
C7—C2—S2	116.24 (11)	C10—C9—C8	119.10 (14)
S3—C2—S2	118.97 (9)	C4—C9—C8	121.67 (13)
C4—C3—S3	114.66 (10)	C11—C10—C9	121.43 (15)
C5—C4—C9	118.86 (14)	C10—C11—C6	119.46 (15)
C5—C4—C3	118.27 (14)		
α′-2			
S1—C1	1.635 (8)	C2—C2^{i}	1.334 (9)
S2—C1	1.719 (4)	C3—C4	1.506 (7)
S2—C2	1.724 (5)	C4—C5	1.376 (6)
S3—C2	1.735 (5)	C4—C4^{i}	1.392 (9)
S3—C3	1.773 (5)	C5—C6	1.380 (7)
C1—S2^{i}	1.719 (4)	C6—C6^{i}	1.384 (12)
C1—S2—C2	97.5 (3)	S2—C2—S3	117.2 (3)
C2—S3—C3	106.2 (2)	C4—C3—S3	115.9 (3)
S1—C1—S2^{i}	123.8 (2)	C5—C4—C4^{i}	119.4 (3)
S1—C1—S2	123.8 (2)	C5—C4—C3	118.6 (5)
S2^{i}—C1—S2	112.4 (4)	C4^{i}—C4—C3	122.1 (3)
C2^{i}—C2—S2	116.20 (16)	C4—C5—C6	121.2 (5)
C2^{i}—C2—S3	126.55 (18)	C5—C6—C6^{i}	119.5 (3)
β-2			
S1*A*—C1*A*	1.642 (3)	S1*B*—C1*B*	1.640 (2)
S2*A*—C1*A*	1.729 (3)	S2*B*—C1*B*	1.732 (3)
S2*A*—C2*A*	1.751 (2)	S2*B*—C2*B*	1.751 (2)
S3*A*—C2*A*	1.747 (2)	S3*B*—C2*B*	1.739 (2)
S3*A*—C3*A*	1.857 (2)	S3*B*—C3*B*	1.842 (3)
S4*A*—C1*A*	1.743 (3)	S4*B*—C1*B*	1.735 (3)
S4*A*—C7*A*	1.748 (2)	S4*B*—C7*B*	1.743 (2)
S5*A*—C7*A*	1.746 (3)	S5*B*—C7*B*	1.747 (2)
S5*A*—C8*A*	1.836 (2)	S5*B*—C8*B*	1.842 (3)
C2*A*—C7*A*	1.353 (3)	C2*B*—C7*B*	1.355 (3)
C3*A*—C4*A*	1.502 (3)	C3*B*—C4*B*	1.506 (3)
C4*A*—C5*A*	1.396 (3)	C4*B*—C5*B*	1.395 (3)
C4*A*—C9*A*	1.404 (3)	C4*B*—C9*B*	1.406 (3)
C5*A*—C6*A*	1.383 (4)	C5*B*—C6*B*	1.383 (4)
C6*A*—C11*A*	1.379 (4)	C6*B*—C11*B*	1.376 (4)
C8*A*—C9*A*	1.496 (3)	C8*B*—C9*B*	1.500 (3)
C9*A*—C10*A*	1.385 (3)	C9*B*—C10*B*	1.392 (3)
C10*A*—C11*A*	1.382 (4)	C10*B*—C11*B*	1.381 (3)
C1*A*—S2*A*—C2*A*	98.25 (12)	C1*B*—S2*B*—C2*B*	98.23 (12)
C1*A*—S2*A*—S4*B*	137.67 (9)	C2*B*—S3*B*—C3*B*	103.42 (11)
C2*A*—S2*A*—S4*B*	103.26 (8)	C1*B*—S4*B*—C7*B*	98.40 (12)
C2*A*—S3*A*—C3*A*	104.81 (11)	C1*B*—S4*B*—S2*A*	149.32 (9)
C1*A*—S4*A*—C7*A*	98.21 (12)	C7*B*—S4*B*—S2*A*	96.82 (8)
C7*A*—S5*A*—C8*A*	103.03 (11)	C7*B*—S5*B*—C8*B*	103.37 (11)
S1*A*—C1*A*—S2*A*	125.05 (17)	S1*B*—C1*B*—S2*B*	125.42 (15)
S1*A*—C1*A*—S4*A*	123.12 (16)	S1*B*—C1*B*—S4*B*	122.83 (16)
S2*A*—C1*A*—S4*A*	111.78 (14)	S2*B*—C1*B*—S4*B*	111.74 (13)
C7*A*—C2*A*—S3*A*	125.47 (19)	C7*B*—C2*B*—S3*B*	125.24 (19)
C7*A*—C2*A*—S2*A*	115.93 (18)	C7*B*—C2*B*—S2*B*	115.63 (18)
S3*A*—C2*A*—S2*A*	118.34 (14)	S3*B*—C2*B*—S2*B*	118.94 (14)

Table 2 (continued)

C4*A*—C3*A*—S3*A*	115.85 (17)	C4*B*—C3*B*—S3*B*	115.48 (18)
C5*A*—C4*A*—C9*A*	118.5 (2)	C5*B*—C4*B*—C9*B*	118.3 (2)
C5*A*—C4*A*—C3*A*	118.7 (2)	C5*B*—C4*B*—C3*B*	118.8 (2)
C9*A*—C4*A*—C3*A*	122.7 (2)	C9*B*—C4*B*—C3*B*	122.9 (2)
C6*A*—C5*A*—C4*A*	121.4 (2)	C6*B*—C5*B*—C4*B*	121.5 (2)
C11*A*—C6*A*—C5*A*	119.5 (2)	C11*B*—C6*B*—C5*B*	120.0 (2)
C2*A*—C7*A*—S5*A*	129.31 (19)	C2*B*—C7*B*—S4*B*	115.76 (18)
C2*A*—C7*A*—S4*A*	115.62 (19)	C2*B*—C7*B*—S5*B*	128.85 (19)
S5*A*—C7*A*—S4*A*	115.07 (14)	S4*B*—C7*B*—S5*B*	115.37 (14)
C9*A*—C8*A*—S5*A*	114.06 (17)	C9*B*—C8*B*—S5*B*	111.83 (17)
C10*A*—C9*A*—C4*A*	119.3 (2)	C10*B*—C9*B*—C4*B*	119.4 (2)
C10*A*—C9*A*—C8*A*	119.5 (2)	C10*B*—C9*B*—C8*B*	119.1 (2)
C4*A*—C9*A*—C8*A*	121.2 (2)	C4*B*—C9*B*—C8*B*	121.5 (2)
C11*A*—C10*A*—C9*A*	121.3 (2)	C11*B*—C10*B*—C9*B*	121.3 (2)
C6*A*—C11*A*—C10*A*	119.8 (2)	C6*B*—C11*B*—C10*B*	119.6 (2)

Symmetry codes: (i) $\frac{3}{2}-x, y-\frac{1}{2}, \frac{1}{2}-z$; (ii) $\frac{3}{2}-x, \frac{1}{2}+y, \frac{1}{2}-z$.

located between the *U* saddle point and the *Z* form. No direct route was found between *Z* and the T_L/T_R conformations. At the saddle point, $U_L \leftrightarrow U_R$ (= *U*), the thione group is somewhat bent towards the phenyl ring. The substitution of Br atoms onto the phenyl ring does not lead to a great change in the difference in energy between the conformations U_L/U_R and *Z* (< 1.25 kJ mol^{-1} in both molecules). Assuming a flat energy surface between the states, a relatively even distribution of conformers would be expected. However, the substitution increases the barrier to conformational inversion by ∼20 kJ mol^{-1} on going from U_L/U_R to *Z* and by ∼70 kJ mol^{-1} on going from *Z* to U_L/U_R, which is probably a steric effect. Conformations T_L and T_R are not affected much by this substitution and both the energy difference and the barrier to inversion remain within ∼2 kJ mol^{-1} of their original values.

3.3. Comparison of X-ray structures

The molecule in the *α*′-(2) polymorph has *m* symmetry, which is perpendicular to and bisects the benzene ring. Atoms S1 and C1 lie on this mirror plane (Fig. 2). The structure of *α*-(2) (Fig. 1), on the other hand, consists of two enantiomeric conformations (one corresponding to the asymmetric unit and one generated by space-group symmetry), in which S1 is displaced from the centroid, towards or away from C5, to give structures which are similar to the U_R and U_L forms calculated in the molecular mechanics study. The U_R- and U_L-type conformations are also observed for each of the two independent molecules of *β*-(2). As modelled here, the molecules of the asymmetric unit of *β*-(2) are both U_L types, but once again the structure is centrosymmetric. The calculated energy barrier for the U_R/U_L interconversion in (2) is only 6.55 kJ mol^{-1} and is therefore readily overcome at room temperature. Thus, if the temperature is high enough, the molecules can librate with interchange of conformation between the U_R and U_L states. It is for this reason that the disorder of structure *α*′-(2), relative to *α*-(2), is considered to be dynamic (librational) rather than static in nature.

In crystallographic terms, the relationship between structures *α*′-(2) and *α*-(2) is simple. The data collection and structure refinement of *α*-(2) was originally carried out in

Table 3
Energies and populations of conformational minima.

	(2)			(3)		
Minima	E_{MM2*} (kJ mol^{-1})	Boltzman factor	Population ratios (300 K)	E_{MM2*} (kJ mol^{-1})	Boltzman factor	Population ratios (300 K)
U_L	−55.22	4.28×10^9	389	−30.21	1.86×10^5	155
U_R	−55.22	4.28×10^9	389	−30.21	1.86×10^5	155
Z	−53.36	2.03×10^9	185	−31.10	2.66×10^5	222
T_L	−40.36	1.10×10^7	1	−17.64	1.20×10^3	1
T_R	−40.36	1.10×10^7	1	−17.64	1.20×10^3	1

Table 4
Energies of saddle points.

Saddle point	(2) E_{MM2*} (kJ mol^{-1})	(3) E_{MM2*} (kJ mol^{-1})
$[U_L \leftrightarrow U_R] = U$	−48.67	−23.06
$[U_L \leftrightarrow T_L]$	−29.15	−6.03
$[U_R \leftrightarrow T_R]$	−29.15	−6.03
$[U \leftrightarrow Z]$	−1.15	43.00

space group $P2_1/c$: subsequent re-refinement, after application of the appropriate cell and Miller index transformations, was carried out in the alternative non-standard setting of $P2_1/a$. This showed that the sizes and shapes of unit cells of α'-(2) and α-(2), neglecting the *C*-centring of the former, and allowing for the effects of thermal expansion, are virtually identical. Furthermore, the addition of a crystallographic mirror plane at $y = 0$ to the structure of α-(2) at 150 K converts the $P2_1/a$ space group into its supergroup $C2/m$, as required for the room-temperature form of α'-(2). As is evident in Figs. 1 and 2, the anisotropic displacement ellipsoids are significantly larger for α'-(2) than for α-(2), but more importantly those of the S atoms are much larger in α'-(2) than in α-(2). A refinement for α'-(2) in which S3 was modelled as being disordered about the mirror plane led to essentially identical residuals.

In Table 2 it is noticeable that despite the larger cell of α'-(2) the bond distances, especially those involving S atoms, are generally shorter than those observed in α-(2), although no corrections for libration have been made. The bond-length differences are not large and not individually statistically significant, but they are consistently in the same sense. It is concluded that the symmetry of the molecule as depicted in α'-(2) arises from the superimposition of the images of the two enantiomeric conformations of α-(2). There is a concern that the comparatively high (*C*-centred) symmetry of α'-(2) has come about due to a failure to measure weak reflections with $h + k$ odd. However, a further data collection using a Bruker SMART 1000 area detector system and paying particular attention to this very point, completely confirmed the choice of the *C*-centred cell for α'-(2). There was little evidence for diffuse scattering in the CCD data frames.

The interchange between U_R and U_L conformations involves rotations about the S3—C3 and S5—C8 bonds. The S1 atom in U_R (or U_L) is displaced from its position in the C_v symmetric U conformation by ∼1/4 of the diameter of a benzene ring, *i.e.* approximately 0.7 Å. The C2—S3—C3—C4 and C7—S5—C8—C9 dihedral angles provide another estimate of the effect. In the U conformation of α'-(2) these angles are equal in magnitude [8.7 (5)°], but opposite in sign. In the conformations in α-(2) these angles are −17.10 (13) and −33.34 (13)°, respectively; the average change in these angles over the six occurrences in the three molecules with U_R/U_L conformations being 25.47°. In the transformation from U_R to U_L, the S1 displacement and the change in dihedral angle each has twice the values given above. Both these measures tend to exaggerate the degree of distortion because the change in value has a component arising from the displacement of the central atoms, especially S3 and S5.

The fact that the change in conformation from U_R to U_L requires no more than bond twisting is further evidence in support of molecular libration as the probable cause of the order–disorder relationship between α'-(2) and α-(2), which in turn is the justification for their α' and α phase designations.

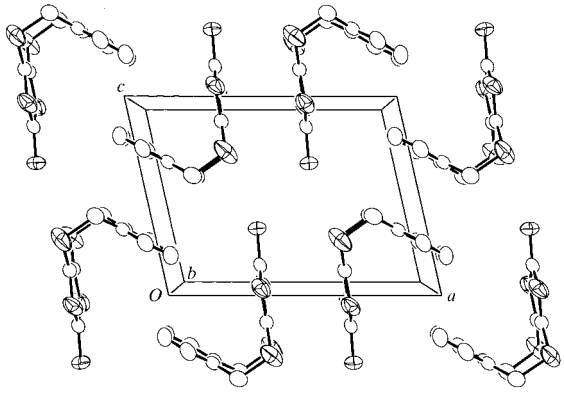

Figure 5
Packing diagram for α'-(2).

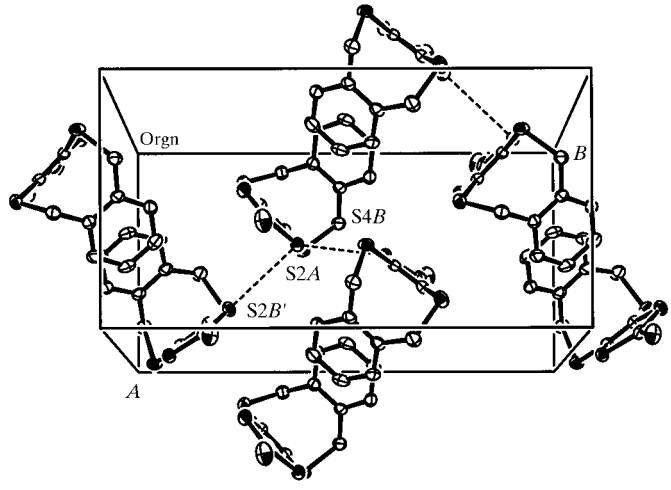

Figure 6
Layer of molecules in β-(2). Dashed lines indicate short S···S contacts (see text).

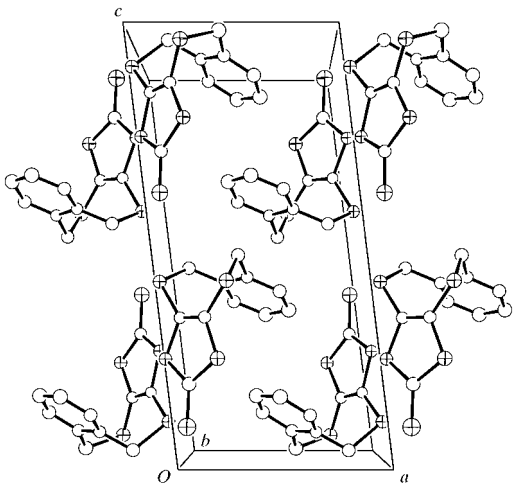

Figure 7
Packing diagram for β-(2).

The packing of the molecules of α'-(2) and α-(2) in their unit cells is essentially the same. As shown in Fig. 4 the molecules of α-(2), when viewed along **b**, lie edge-on, forming layers centred on $y = 0$ and $y = 1/2$. Within the layers, both the benzene rings and the dmit moieties occur face-to-face in centrosymmetrically related pairs. In α'-(2) (Fig. 5), the perpendicular distances between benzene ring pairs, centred on 0,0,0 and 0,0,1/2, are 3.276 (14) and 3.544 (8) Å, respectively, while the perpendicular distance between the dmit planes defined by the C2═C7 double bond and its attached S atoms is 3.748 (4) Å. In α-(2), the corresponding distances are 2.959 (5), 3.554 (4) and 3.630 (6) Å.

Despite both molecules in the asymmetric unit having conformations essentially the same as in α-(2), the packing of the molecules in the β-(2) phase is completely different. As shown in Fig. 6, the molecules occur in *AB* pairs, arranged in a herringbone-type array, to form a layer parallel to (001) and with z in the range 0–1/2. Short S···S contacts of 3.3259 (9) Å [S2*A*···S4*B*] and 3.5568 (9) Å (S2*A*···S2*B*′) occur between the pairs of molecules. A second layer, related to the first by the operation of a crystallographic centre of symmetry, completes the unit-cell contents. Centrosymmetric face-to-face benzene ring contacts occur from one layer to the next at $z = 0$ and 1/2 (see Fig. 7) at perpendicular distances of 3.537 (3) [*AA* pairs] and 3.574 (3) Å [*BB* pairs]. In contrast, there are no face-to-face contacts of the dmit moieties within the sum of the van der Waals' radii for two S atoms (3.70 Å; Huheey *et al.*, 1993). It is the gross difference in molecular packing which prompts the designation of β-(2) as a true polymorph.

The molecules of β-(2) can be regarded as forming a column comprising non-centrosymmetric *AB* molecule pairs, centred on $z = 1/4$ and 3/4, each pair being related to the next by a crystallographic centre of symmetry at $z = 0$ or 1/2. Similar columns are also present in α-(2) and α'-(2), but they are less obvious: here the equivalent of the *AB* molecule pairs of β-(2) are centrosymmetric, the columns are propagated in the *a* direction and arranged side by side in the *c* direction in such a way as to create centrosymmetrically related pairs of dmit moieties and so complete the layers.

We thank the EPSRC National Crystallography Service (University of Southampton) for data collections.

References

Allen, F. H. & Kennard, O. (1993). *Chem. Des. Autom. News*, **8**, 31–37.
Blessing, R. H. (1997). *J. Appl. Cryst.* **30**, 421–426.
Culot, P., Dive, G., Nguyen, V. H. & Ghuysen, J. M. (1990). *Theoret. Chim. Acta*, **82**, 189–205.
Desiraju, G. R. (1995). *Angew. Chem. Int. Ed. Engl.* **34**, 2311–2327.
Fletcher, D. A., McMeeking, R. F. & Parkin, D. (1995). *J. Chem. Inf. Comput. Sci.* **36**, 746–749.
Goldenberg, L. M. & Lyubovskaya, R. N. (1986). *Khim. Geterotsikl. Soed.* **6**, 855–856.
Hooft, R. W. W. (1998). *Collect.* Enraf–Nonius, Delft, The Netherlands.
Howie, R. A. (1980) *RDNIC.* University of Aberdeen, Scotland.
Huheey, J. E., Keiter, E. A. & Keiter, R. L. (1993). *Inorganic Chemistry, Principles of Structure and Reactivity*, 4th ed. New York: HarperCollins.
Hunter, C. A. (1994). *Chem. Soc. Rev.* **23**, 101–109.
Kumar, S. K., Singh, H. B., Jasinski, J. P., Paight, E. S. & Butcher, R. J. (1991). *J. Chem. Soc. Perkin Trans 1*, pp. 3341–3347.
Mohamadi, F., Richards, N. G. J., Guida, W. C., Liskamp, R., Lipton, M., Caulfield, C., Chang, G., Hendrickson, T. & Still, W. C. (1990). *J. Comput. Chem.* **11**, 440–467.
Nicolet Instrument Corporation (1980). *P*3 *Software.* Nicolet Instrument Corporation, Madison, Wisconsin, USA.
Otwinowski, Z. & Minor, W. (1997). *Methods Enzymol.* **276**, 307–326.
Sheldrick, G. M. (1990). *Acta Cryst.* A**46**, 467–473.
Sheldrick, G. M. (1997). *SHELXL*97. University of Göttingen, Germany.
Still, W. C., Tempczyk, A., Hawley, R. C. & Hendrickson, T. (1990). *J. Am. Chem. Soc.* **112**, 6127–6129.
Wang, C., Batsanov, A. S., Bryce, M. R. & Howard, J. A. K. (1998). *Synthesis*, pp. 1615–1618.